Interplay between surface anisotropy and dipolar interactions in an assembly of nanomagnets

Z. Sabsabi,[1] F. Vernay,[1,*] O. Iglesias,[2,†] and H. Kachkachi[1]

[1]*Laboratoire PROMES-CNRS UPR 8521 & Université de Perpignan Via Domitia, Rambla de la Thermodynamique–Tecnosud, 66100 Perpignan, France*

[2]*Dept. de Física Fonamental and Institute of Nanoscience and Nanotechnology (IN2UB), Facultat de Física, Universitat de Barcelona, Av. Diagonal 647, 08028 Barcelona, Spain*

(Received 1 July 2013; revised manuscript received 9 September 2013; published 25 September 2013)

We study the interplay between the effects of surface anisotropy and dipolar interactions in monodisperse assemblies of nanomagnets with oriented anisotropy. We derive asymptotic formulas for the assembly magnetization, taking into account temperature, applied field, core and surface anisotropy, and dipolar interparticle interactions. We find that the interplay between surface anisotropy and dipolar interactions is well described by the analytical expression of the assembly magnetization derived here: the overall sign of the product of the two parameters governing the surface and the dipolar contributions determines whether intrinsic and collective terms compete or have synergistic effects on the magnetization. This is illustrated by the magnetization curves of γ-Fe_2O_3 nanoparticle assemblies in the low concentration limit.

DOI: 10.1103/PhysRevB.88.104424 PACS number(s): 75.75.Fk, 75.50.Tt, 75.30.Gw

I. INTRODUCTION

Assemblies of magnetic nanoparticles, deposited on a substrate or embedded in a matrix, provide a very rich laboratory for various investigations, experimental and theoretical, with stimulating challenges both for fundamental research and practical applications.[1–5] An issue of particular importance is that of the interplay between intrinsic features of the nanomagnet pertaining to their finite-size and boundary effects, and the collective effects induced by their mutual interactions and their interactions with the hosting matrix or substrate.[6–10]

Experimental studies are numerous as they have concerned a variety of parameters, such as the production methods, particle sizes, shapes and surface, matrices and substrates, degrees of concentration, organization, and aggregation.[3,6–8,11–22] In particular, in some studies a subtle interplay was revealed between the effects of the size distribution and the concentration of assemblies. The results seem to hint at a kind of screening of the intrinsic effects by the interparticle interactions in dense assemblies. For example, measurements of the magnetization at high fields performed on the γ-Fe_2O_3 nanoparticles[8,23] and on cobalt particles[6] showed that the magnetization is strongly influenced by surface effects. To be more explicit, Figs. 3 and 5 of Ref. 8 together with Fig. 1 of Ref. 24 represent magnetization curves for assemblies of maghemite nanoparticles with different concentrations. One clearly sees that the $M(H)$ curves at different temperatures present a rather different behavior as one compares dilute with concentrated assemblies. Furthermore, measurements of the temperature T_{max} at the maximum of the zero-field-cooled (ZFC) magnetization as a function of the applied magnetic field change from a bell-like curve for dilute assemblies into a monotonous decreasing function of the magnetic field for concentrated systems.[25] As of today, the situation has not changed very much regarding our understanding of the phenomena observed in these experiments and many others. From a theoretical point of view, the situation involving both acute surface effects and long-ranged dipolar interactions has never been investigated in detail so far mainly because of its tremendous complexities. In this context, there are several contributions using either (semi)analytical approaches based on thermodynamic perturbation theory or mean-field theory, or numerical studies such as the integration of the Fokker-Planck equation or Monte Carlo simulations.[22,26–37]

The dynamics of an assembly of magnetic nanoparticles, even weakly interacting, is still another far more complex and challenging problem. During the past two decades, several models have been proposed to tackle this issue with a special focus on the effects of dipole-dipole interactions (DDIs) on the distribution of the energy barriers and of the relaxation rates and the related dynamical observables such as the ac susceptibility. One can find in the literature many contradictory results as to whether DDIs contribute to enhance or to decrease the energy barrier of an interacting nanoparticle.[14,30,31,36,38–45] In Ref. 29 it was pointed out that these discrepancies are mainly due to the fact that the discussions only focus on the "static" effect of DDIs on the uniaxial energy potential and thus overlook the fact that it is not only the energy landscape that is important but also how the magnetic moment evolves in it and how strongly its motion is damped. Indeed, the presence of transverse components of the local effective fields creates a saddle point in the uniaxial potential barrier of the individual magnetic moments, and this makes the relaxation rate sensitive to damping. Unfortunately, dealing with damping effects for studying the dynamics of an interacting assembly of magnetic moments by, e.g., computing the relaxation rate(s) of the assembly is a tremendous task which will still trigger many investigations in the years to come. In this context, the relaxation rate of the simplest nontrivial model of two magnetic moments coupled by DDIs has been computed in a study that has revealed several switching mechanisms.[46]

Real systems are assemblies of many-spin nanoparticles. On the other hand, the investigation of surface effects requires an approach that accounts for the internal structure of the nanoparticle regarded as a nanocrystal of many atomic spins. Unfortunately, a system of interacting many-spin particles is beyond the reach of any analytical calculation and is horrendously difficult for numerical simulations. A compromise has

been suggested in Ref. 47, where it is shown that a many-spin particle can be modeled by a macroscopic magnetic moment (the so called macrospin) evolving in an effective potential that captures the main intrinsic features of the nanoparticle pertaining to its size, shape, underlying lattice, and spin-spin interactions. This potential comprises contributions that stem from the core and surface anisotropies of the particle with coefficients whose sign and magnitude depend on the intrinsic features.[48–50] Therefore, this effective model then allows us to represent the magnetic state of a nanoparticle by a single macroscopic magnetic moment while taking into account to some extent the intrinsic properties. Consequently, a dilute assembly of the so-represented nanoparticles provides a system of weakly interacting magnetic moments each evolving in an effective potential. Hence, one can deal with such a system using thermodynamic perturbation theory with respect to the (weak) DDIs where the thermodynamic averages are computed with respect to the Gibbs distribution for the effective potential energy.

Therefore, in the sequel we will consider and refer to the following models:

(i) The one-spin problem (OSP), also known as the macrospin approximation: each magnetic particle is modeled by a single magnetic moment, corresponding to the net magnetic moment of the cluster, evolving in an energy potential that comprises Zeeman and anisotropy contributions. Usually, the anisotropy is uniaxial and incorporates the shape anisotropy as well.

(ii) The effective one-spin problem (EOSP): in this model, a many-spin magnetic particle, inherently exhibiting surface anisotropy, can equivalently be described by a single magnetic moment where surface effects are taken into account by an effective potential.

Then the task of the present work is to derive asymptotic analytical expressions for the magnetization as a function of temperature and applied field, which include contributions from the magnetic field, core and surface anisotropies, and DDIs. Upon varying the physical parameters of the assembly, such as its shape (oblate or prolate) and concentration, it is possible to investigate the competition between surface anisotropy and interparticle interactions. To investigate this competition without interference of other parameters such as the volume and the easy axis distributions, we restrict our study to monodisperse assemblies with oriented anisotropy with all easy axes pointing in the direction of the applied field.

In Ref. 35, the interplay between the effects of surface anisotropy and DDIs was also studied using the same approach with a computing method that consisted in a numerical calculation of the integrals that yield the magnetization for individual particles. A comparison with Monte Carlo calculations for arbitrary strength of DDIs was also presented. The present work is an important addition in that it focuses on the analytical expressions for the magnetization. More precisely, one of the major goals here is to provide practical analytical expressions for the magnetization that take into account the applied magnetic field, the (core) uniaxial anisotropy, the (surface) cubic anisotropy, DDIs, and temperature. This is indeed achieved in limiting cases for the field, surface anisotropy, and DDIs. This analytical tool allows us to discuss in more detail the competition between intrinsic and collective effects, and is useful for a simple fitting procedure of experimental data on dilute assemblies of rather small particles with identified surface effects. The present results can also be helpful in optimizing the physical parameters for new experimental studies of nanoparticles assemblies in view of a better understanding of the physical phenomena discussed above and eventually for the practical applications in vogue nowadays, especially those which target a functionalization of the particle surface.

After this Introduction, the paper is organized in five sections: the OSP and EOSP models and the corresponding general expression for the magnetization are presented in Sec. II. Next, Sec. III is devoted to the derivation of low-field asymptotes, in the high- and low-anisotropy limits, for the assembly magnetization. These analytical expressions provide a link to previous studies and highlight the effect of the shape of the assembly on the magnetization when only the DDIs are taken into account. The competition between intrinsic and long-range terms in the energy is then investigated in Sec. IV, where the magnetization of the assembly within the EOSP approach is derived. The analytical expressions computed in these last two sections are then discussed in detail in Sec. V. The paper ends with some concluding remarks and outlook.

II. MODEL AND PHYSICAL OBSERVABLES

A. Energy

We consider an assembly of $\mathcal{N}$ ferromagnetic nanoparticles, each carrying a magnetic moment $\mathbf{m}_i = m_i \mathbf{s}_i$, $i = 1, \ldots, \mathcal{N}$ of magnitude m_i and direction $\mathbf{s}_i$, with $|\mathbf{s}_i| = 1$. $\mathbf{m}_i$ is then measured in terms of the Bohr magneton μ_B, i.e., $m_i = n_i \mu_B$, and n_i are either all equal for monodisperse assemblies or chosen according to some distribution, the so-called polydisperse assemblies. Each magnetic moment has a uniaxial easy axis $\mathbf{e}_i$, and for an assembly these may be either all directed along some reference axis leading to an oriented assembly, or randomly distributed. The former situation is the one that we consider here, and we will refer to it as oriented anisotropy (OA). Hence, the energy of a magnetic moment $\mathbf{m}_i$ interacting with the whole assembly reads (after multiplying by $-\beta = -1/k_B T$)

$$\mathcal{E}_i = \mathcal{E}_i^{(0)} + \mathcal{E}_i^{\mathrm{DDI}}, \tag{1}$$

where the first contribution

$$\mathcal{E}_i^{(0)} = x_i \mathbf{s}_i \cdot \mathbf{e}_h + \mathcal{A}(\mathbf{s}_i)$$

is the energy of the free nanoparticle at site i with the first term being the Zeeman energy with the magnetic field having the verse $\mathbf{e}_h$. The second term is the anisotropy contribution, where $\mathcal{A}(\mathbf{s}_i)$ is a function that depends on the anisotropy model and is given by

$$\mathcal{A}(\mathbf{s}_i) = \begin{cases} \sigma_i (\mathbf{s}_i \cdot \mathbf{e}_i)^2, & \text{OSP} \\ \sigma_i \left[(\mathbf{s}_i \cdot \mathbf{e}_i)^2 - \frac{\zeta}{2} \left(s_{i,x}^4 + s_{i,y}^4 + s_{i,z}^4 \right) \right], & \text{EOPS.} \end{cases} \tag{2}$$

As the main purpose of the present paper is to develop analytical expressions, we restrict ourselves to textured samples where the uniaxial anisotropies of Eq. (2) remain along the

external magnetic field, i.e., $\mathbf{e}_i \parallel \mathbf{e}_h$. Moreover, in the second line of Eq. (2) we assume the simplest situation in which the three axes of the cubic anisotropy coincide with the crystal axes and that one of them coincides with the easy axis of the uniaxial anisotropy.

Within the EOSP model, on-site surface anisotropy of the quadratic kind, such as the transverse or Néel models, induces a quartic contribution in the effective energy of the net magnetic moment, under the condition that spin noncolinearities are not too strong.[47] Later it was shown that[49,50] in fact the effective energy of the many-spin particle is a polynomial in the components of its net magnetic moment. This polynomial can be, with a fairly good approximation, limited to a sum of a quadratic and a quartic contribution with coefficients that change in sign and magnitude with the intrinsic properties of the particle, namely its size, shape, underlying lattice structure, and physical parameters such as the exchange coupling and on-site core and surface anisotropy. This has been checked numerically in Refs. 48 and 49.

For convenience, in Eqs. (1) and (2) we have introduced the dimensionless parameters

$$\begin{aligned} x_i &\equiv \frac{n_i \mu_B H}{k_B T} = n_i x_0, \\ \sigma_i &\equiv \frac{K_2 V_i}{k_B T} = \frac{(\mu_B/M_s)\, K_2}{k_B T} n_i = \sigma_0 n_i, \\ \zeta &\equiv \frac{K_4}{K_2}. \end{aligned} \tag{3}$$

$\mathbf{H} = H\mathbf{e}_h$ is the external magnetic field, V_i is the volume of the nanoparticle, and K_2 and K_4 are, respectively, the quadratic and quartic anisotropy constants. Since we are considering assemblies with moment instead of volume distribution, the volume V_i may be rewritten in terms of n_i via the saturation magnetization of the material per unit volume M_s, i.e., $V_i = m_i/M_s = (\mu_B/M_s)n_i$.

In addition to the intrinsic contributions to the energy, the expression in Eq. (1) also includes a contribution stemming from DDIs which reads

$$\begin{aligned} \mathcal{E}_i^{\mathrm{DDI}} &= \sum_{j<i} \xi_{ij} \frac{3(\mathbf{s}_i \cdot \mathbf{e}_{ij})(\mathbf{s}_j \cdot \mathbf{e}_{ij}) - \mathbf{s}_i \cdot \mathbf{s}_j}{r_{ij}^3} \\ &= \sum_{j<i} \xi_{ij} \mathbf{s}_i \cdot \mathcal{D}_{ij} \cdot \mathbf{s}_j \end{aligned} \tag{4}$$

with the corresponding dimensionless DDI coupling

$$\xi_{ij} = \left(\frac{\mu_0}{4\pi}\right)\left(\frac{\mu_B^2 n_i n_j/a^3}{k_B T}\right). \tag{5}$$

$\mathcal{D}_{ij}$ is the DDI tensor,

$$\mathcal{D}_{ij} \equiv \frac{1}{r_{ij}^3}(3\mathbf{e}_{ij}\mathbf{e}_{ij} - 1) \quad \text{with} \quad \mathbf{r}_{ij} = \mathbf{r}_i - \mathbf{r}_j,\ \mathbf{e}_{ij} = \frac{\mathbf{r}_{ij}}{r_{ij}}. \tag{6}$$

For the sake of clarity of our discussions of the competition between intrinsic and collective effects, we will assume that the nanoparticles are distributed on a stereotypical simple-cubic superlattice with lattice parameter a. Therefore, the vector $\mathbf{r}_{ij}$ connects the sites i and j and its magnitude is measured in units of a.

It is useful to give some orders of magnitude for the DDI strength in nanoparticle assemblies. For example, a cobalt atom carries a magnetic moment of $n_0 \simeq 1.7$ Bohr magnetons. For two such atoms separated by the atomic distance $a_0 = 0.3554$ nm, $\xi = \frac{1}{k_B T}(\frac{\mu_0}{4\pi})(\mu_B^2 n_0^2/a_0^3) \simeq 0.004$ at 10 K. A nanoparticle of diameter $D = 3$ nm contains about $n \simeq 2172$ of such atoms. For two such particles separated by a distance of $3D$, we have at the same temperature $\xi \simeq 1.17$, which is three orders of magnitude larger than for atoms.

Finally, let us relate the DDI parameter to the real assembly parameters, especially the concentration of nanoparticles in a hosting matrix. From the form of the DDI tensor $\mathcal{D}_{ij}$ in Eq. (6), it appears that DDIs depend on two parameters: the interparticle distance and the relative orientation of the particles. The DDI strength can equivalently be characterized by the parameter ξ or the volume concentration C_{v}, which can be written as[26]

$$C_{\mathrm{v}} = p\left(\frac{k_{\mathrm{lat}}\pi}{6}\right)\left(\frac{D}{a}\right)^3, \tag{7}$$

where a is the lattice constant introduced earlier, D is the particle diameter, and k_{lat} is a constant that depends on the lattice structure. For instance, for a simple-cubic lattice, $k_{\mathrm{lat}} = 1$. p represents the occupancy probability of a lattice site, which for the present case is $p = 1$. Then, C_{v} and ξ are related as follows:

$$\xi = \left(\frac{\mu_0}{4\pi}\right)\frac{(\mu_B n)^2}{k_B T}\frac{6}{\pi D^3} C_{\mathrm{v}} = \frac{T_0}{T}\left(\frac{D}{a_0}\right)^3 C_{\mathrm{v}}$$

with T_0 and a_0 being constants corresponding, respectively, to an arbitrary temperature and a length such that the ratio T_0/a_0^3 is given by

$$\frac{T_0}{a_0^3} = \frac{\mu_0 \mu_B^2}{24 k_B}\alpha^2,$$

where α represents the number of Bohr magnetons per unit volume.

On the other hand, the presence of the unit vectors $\mathbf{e}_{ij}$ in Eq. (4) implies that the dipolar interaction depends explicitly on the geometry of the sample. To illustrate this effect, we will consider two kinds of assemblies of $\mathcal{N} = 2000$ particles: an oblate sample of dimensions $(20 \times 20 \times 5)$ and a prolate sample $(10 \times 10 \times 20)$.

B. Magnetization

The competition between intrinsic and collective effects in nanomagnet assemblies affects most of the physical properties of the system inducing a modification of various physical observables. In the present work, we choose to focus on equilibrium properties and we therefore investigate the behavior of the magnetization curves $M(H)$, taking into account DDIs.

In Ref. 32 it was shown that in a dilute assembly, the magnetization of a nanocluster at site i (weakly) interacting with the other clusters of the assembly is given (to first order in ξ) by

$$\langle s_i^z \rangle \simeq \langle s_i^z \rangle_0 + \sum_{k=1}^{\mathcal{N}} \xi_{ik} \langle s_k^z \rangle_0 A_{ki} \frac{\partial \langle s_i^z \rangle_0}{\partial x_i}, \tag{8}$$

where $A_{kl} = \mathbf{e}_h \cdot \mathcal{D}_{kl} \cdot \mathbf{e}_h$. $\langle\cdot\rangle$ is the statistical average of the projection on the field direction of the particle's magnetic moment.

Equation (8) was obtained for an external magnetic field applied in the z direction leading to $\langle s_i^{x,y}\rangle_0 = 0$. It is only valid for a center-to-center interparticle distance larger than thrice the mean diameter of the nanoparticles.[33] This implies that the magnetization of an interacting cluster is written in terms of its "free" (with no DDIs) magnetization and susceptibility, with of course the contribution of the assembly "lattice" via the lattice sum in Eq. (8). Therefore, one first has to compute the magnetization of the free cluster.

For an assembly of free particles, it remains relatively straightforward to derive an expression for the free magnetization, $m_i^{(0)} \equiv \langle s_i^z\rangle_0$, for the specific case of uniaxial anisotropy corresponding to the first line of Eq. (2), i.e., the OSP model.[31,32,51] From this expression of $m^{(0)}$, it is then easy to derive, using Eq. (8), an analytical expression for the assembly magnetization that takes into account the DDI in the dilute limit. Furthermore, as will be shown in Sec. IV, an explicit expression for $m^{(0)}$ allows one to derive a perturbative expression for the magnetization for the EOSP by including the cubic anisotropy term with the coefficient ζ as an expansion parameter.

As mentioned earlier, here we restrict ourselves to monodisperse assemblies so as to investigate the interplay between intrinsic and collective effects in pure form. Consequently, we set $x_i = x$, $\sigma_i = \sigma$, and $\xi_{ij} = \xi$. In this case, the magnetization of a (weakly) interacting particle is given by Eq. (8), which now simplifies into the following expression:

$$\langle s^z\rangle \simeq m^{(0)}\left[1 + \xi\mathcal{C}^{(0,0)}\frac{\partial m^{(0)}}{\partial x}\right]. \tag{9}$$

The lattice sum $\mathcal{C}^{(0,0)}$ is in fact the first of a hierarchy of lattice sums.[32] For large samples, $\mathcal{C}^{(0,0)}$may be rewritten in term of the demagnetizing factor D_z along z,[31]

$$\mathcal{C}^{(0,0)} = -4\pi\left(D_z - \frac{1}{3}\right).$$

In the continuum limit and for box-shaped samples of semiaxes a, b, and c, D_z can itself be expressed as follows:

$$D_z = \frac{abc}{2}\int_0^\infty \frac{ds}{(c^2+s)\sqrt{(a^2+s)(b^2+s)(c^2+s)}}.$$

This form of $\mathcal{C}^{(0,0)}$ allows one to have a direct evaluation for large samples of the demagnetizing factor D_z known for different sample aspect ratios.[52]

It then turns out that the relevant DDI parameter, to this order of approximation, is in fact

$$\tilde{\xi} \equiv \xi\mathcal{C}^{(0,0)} = \frac{\xi}{\mathcal{N}}\sum_{i,j=1,i\neq j}^{\mathcal{N}} A_{ij}.$$

Next, the longitudinal susceptibility $\chi_\parallel^{(0)} = \partial m^{(0)}/\partial x$ is given by [see, e.g., Ref. 51 for a review]

$$\frac{\partial m^{(0)}}{\partial x} = \frac{1+2S_2}{3} - (m^{(0)})^2 = a_0^{(1)} - (m^{(0)})^2$$

and thereby we obtain the approximate expression for the magnetization of a particle taking into account DDIs with the other particles in the assembly,

$$\langle s^z\rangle \simeq m^{(0)}\left\{1 + \tilde{\xi}\left[a_0^{(1)} - (m^{(0)})^2\right]\right\}. \tag{10}$$

The free-particle magnetization $m^{(0)}$ can be computed in various ways, either numerically or analytically. Our major concern in this work is to provide ready-to-use analytical expressions for the magnetization of an assembly, including DDIs and surface effects. For this purpose, we adopt an analytical approach with the understanding that this can only be performed in some limiting cases of the applied field and quartic contribution to the particle's anisotropy, i.e., low and high fields and/or small ζ.

Obviously, in the absence of any interaction and anisotropy, or at high temperature, the magnetization is described by the Langevin function

$$\langle s^z\rangle_0(\sigma = 0, \xi = 0) = \mathcal{L}\left(\frac{\mu_0 H M_S}{k_B T}\right), \tag{11}$$

where μ_0 is the vacuum permeability introduced so that $\mu_0 H$ can be measured in teslas.

III. ASSEMBLY OF OSP NANOCLUSTERS: ORIENTED UNIAXIAL ANISOTROPY VERSUS DDIs

In the case of a nanocluster with effective uniaxial anisotropy in a longitudinal magnetic field, i.e., $\mathbf{e}_i \parallel \mathbf{e}_h \parallel \mathbf{e}_z$, the energy reads (dropping the particle's index i)

$$\mathcal{E}^{(0)} = \sigma s_z^2 + x s_z.$$

Then, we introduce the "free" probability distribution

$$\mathcal{P}_0(z) = \frac{1}{Z_\parallel^{(0)}} e^{\mathcal{E}^{(0)}}, \quad Z_\parallel^{(0)}(\sigma, x) = \int_{-1}^{1} ds_z\, e^{\mathcal{E}^{(0)}} \equiv \int d\omega^{(0)}. \tag{12}$$

The free partition function $Z_\parallel^{(0)}$ may then be rewritten in terms of the Dawson integral $D(x) = e^{-x^2}\int_0^x dt\, e^{t^2}$ as[51]

$$Z_\parallel^{(0)}(\sigma, x) = \frac{e^\sigma}{\sqrt{\sigma}}\left[e^x D(\sqrt{\sigma_+}) + e^{-x} D(\sqrt{\sigma_-})\right],$$

where the reduced field $h = x/2\sigma$ and energy barriers $\sigma_\pm \equiv \sigma(1 \pm h)^2$ have been introduced.

The magnetization in the presence of anisotropy and a longitudinal field is then given by

$$\langle s^z\rangle_0(\sigma \neq 0, \xi = 0) = \frac{e^\sigma}{\sigma Z_\parallel^{(0)}}\sinh x - h = \mathcal{C}_1. \tag{13}$$

$\mathcal{C}_1$ is defined in the Appendix.

Now, before using this expression in Eq. (10) to derive the corresponding expression for the assembly magnetization, we recall some asymptotes for the magnetization of the free cluster in various regimes of the anisotropy and applied field. The details of the calculations and more asymptotes can be found in Ref. 51.

First, from Eq. (13) one derives low- and high-anisotropy asymptotes,

$$m^{(0)} \simeq \begin{cases} \mathcal{L}(x) + \frac{2}{x}\left\{\mathcal{L}^2(x) - \left[1 - \frac{3}{x}\mathcal{L}(x)\right]\right\}\sigma, & \sigma \ll 1, \\ \tanh x\left[1 - \frac{1}{2\sigma}\left(1 + \frac{2x}{\sinh(2x)}\right)\right], & \sigma \gg 1 \end{cases}$$

and similarly for the longitudinal susceptibility we get

$$\frac{\partial m^{(0)}}{\partial x} \simeq \begin{cases} \frac{1}{3} - \mathcal{L}^2(x) + 4\left\{\frac{1}{45} - \frac{\mathcal{L}(x)}{x}\left\{\mathcal{L}^2(x) - \left[1 - \frac{3}{x}\mathcal{L}(x)\right]\right\}\right\}\sigma, & \sigma \ll 1, \\ (1 - \tanh^2 x) - \left[1 - \tanh^2 x\left(1 + \frac{2x}{\sinh(2x)}\right)\right]\frac{1}{\sigma}, & \sigma \gg 1. \end{cases}$$

Since the present investigation focuses on the collective equilibrium behavior in the low-temperature limit, we note in passing that typical physical parameters of (metallic or oxide) nanoparticles are such that $\sigma \gg 1$.

Next, for the assembly we use Eq. (10) to derive the low- and high-field asymptotes in both anisotropy regimes. For low fields, we use the low-field expansion of the Langevin function [$\mathcal{L}(x) \simeq \frac{x}{3} - \frac{x^3}{45}$] to get the low-field asymptotes for the assembly magnetization,

$$\langle s^z \rangle_{\rm LF} \simeq \begin{cases} m^{(0)}\left[1 + \tilde{\xi}\left(\frac{1}{3} + \frac{4}{45}\sigma\right)\right], & \sigma \ll 1, \\ m^{(0)}\left[1 + \tilde{\xi}\left(1 - \frac{1}{\sigma}\right)\right], & \sigma \gg 1. \end{cases}$$

For high fields, we have $\mathcal{L}(x) \simeq 1 - \frac{1}{x}$, which leads to the following asymptotes:

$$\langle s^z \rangle_{\rm HF} \simeq \begin{cases} m^{(0)}\left[1 + \tilde{\xi}\left\{\left(-\frac{2}{3} + \frac{4}{45}\sigma\right) + \frac{2}{x}\right\}\right], & \sigma \ll 1, \\ m^{(0)}\left[1 + \tilde{\xi}\, O\left(\frac{1}{\sigma^2}\right)\right], & \sigma \gg 1. \end{cases}$$

The magnetization and thermal averages of higher-order moments are given in the Appendix.

While the previous low-field and high-field asymptotes for the magnetization are useful for various estimations, one can of course use the exact semianalytical expression of Eq. (13), insert it in Eq. (10), and obtain the magnetization for the whole range of the applied field. The result of this procedure is shown in Fig. 1.

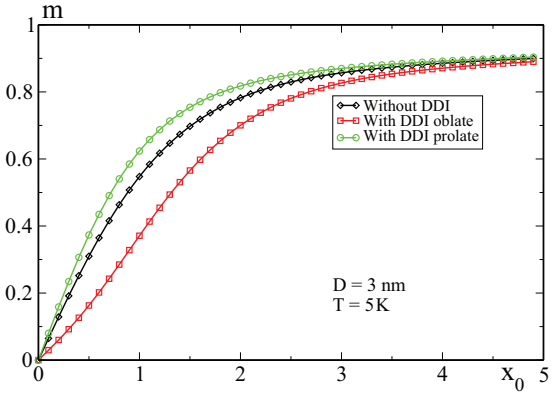

FIG. 1. (Color online) Reduced magnetization of two assemblies of equivalent sizes, of prolate and oblate shape, with ($\tilde{\xi} = 0.18$) or without ($\tilde{\xi} = 0$) a DDI.

Here the effect of DDIs and of the sample's shape is obvious. As is well known (see, e.g., Ref. 32 and references therein), DDIs are anisotropic interactions and thus contribute to the effective anisotropy. Since the anisotropy is uniaxial and oriented, i.e., with a common easy axis, its effect leads to a magnetization enhancement. On the contrary, the DDI effect depends on the sign of $\tilde{\xi}$ (or more precisely that of $\mathcal{C}^{(0,0)}$), which is directly related to the sample's shape. For instance, in the case of oblate samples, $\mathcal{C}^{(0,0)} < 0$ leading to a reduction of the magnetization, while for prolate samples, $\mathcal{C}^{(0,0)} > 0$ and thereby DDIs contribute to the enhancement of the assembly's magnetization. Consequently, for oblate samples the (oriented) uniaxial anisotropy and DDIs have opposite effects while for prolate samples they play concomitant roles.

The integral of $Z_{\parallel}^{(0)}$ in Eq. (13) may also be extended to include the quartic contribution to the energy potential and thereby deal with surface anisotropy and its competition with DDIs. This will be shown in the next section. The numerical calculations of the integral of $Z_{\parallel}^{(0)}$ were done in Ref. 35.

IV. ASSEMBLY OF EOSP CLUSTERS: SURFACE ANISOTROPY VERSUS DDIs

The aim of this section is to deal with (weakly) interacting assemblies of EOSP particles and investigate the interplay between surface anisotropy and DDIs. This means that in addition to the uniaxial anisotropy and Zeeman contributions, the free-particle energy also includes a quartic contribution in the components of its net magnetic moment according to the second line of Eq. (2). This effective potential comprises a cubic anisotropy contribution, with the coefficient ζ,[47–50] that accounts for the surface anisotropy. The latter is initially modeled in the many-spin description of a nanocluster with the help of Néel's model for atomic spins.

Making use of the condition $\|s\| = 1$, the cubic-anisotropy energy that is usually written as

$$E_{\rm CA} = -K_4 V\left(s_x^2 s_y^2 + s_z^2 s_y^2 + s_x^2 s_z^2\right) \tag{14}$$

can be recast in the more compact expression (upon dropping an irrelevant constant) $E_{\rm CA} = \frac{K_4 V}{2}\sum_{\alpha=x,y,z} s_\alpha^4$. Then, using the notation in Eq. (2) we define the (dimensionless) energy $\mathcal{E}_{\rm CA} = \frac{\zeta}{2}\sum_{\alpha=x,y,z} s_\alpha^4$. For later discussion, we recall that depending on the sign of ζ, there are different easy axes:

(i) If $\zeta > 0$, there are 8 minima, 12 saddle points, and 6 maxima. The easy axes lie along the main diagonal of the cube.

(ii) If $\zeta < 0$, there are 6 minima, 12 saddle points, and 8 maxima. The easy axes are along (Ox), (Oy), and (Oz).

A. Surface effects in the absence of DDIs

First we would like to highlight the effect of surface anisotropy on the magnetization curves. So here we compute the magnetization without the DDI contribution (i.e., $\xi = 0$). Hence, the partition function is given by

$$Z = \int d\varphi\, d\omega^{(0)} e^{-\frac{\sigma\zeta}{2}\sum_{\alpha=x,y,z} s_\alpha^4}.$$

Then, we assume that the cubic anisotropy is small. Indeed, the condition of validity for the EOSP model[47–50] obtained for a nanocluster with an SC crystal lattice is $\zeta = K_4/K_2 \lesssim 1/4$ ($\zeta \lesssim 0.35$ for an fcc lattice). In this case, the spin noncolinearities induced by surface anisotropy are supposed to be not too strong, and thereby the anisotropy energy minima are mainly determined by the uniaxial contribution, whereas the cubic contribution only introduces saddle points. This leads to larger relaxation rates[53] but does not affect the physical properties at equilibrium.

Consequently, it is quite legitimate to expand the partition function Z in terms of ζ leading to

$$Z \simeq Z_\parallel^{(0)} - \frac{\sigma\zeta}{2}(Z_\parallel^{(2)} + Z_\perp^{(2)}), \tag{15}$$

where the "longitudinal" partition functions $Z_\parallel^{(0)}$ and $Z_\parallel^{(2)}$ are defined in Eqs. (12) and (A4), while the transverse component $Z_\perp^{(2)}$ is given by

$$Z_\perp^{(2)} = \int d\varphi \left(s_x^4 + s_y^4\right) d\omega^{(0)}.$$

Next, by symmetry we have $\langle s_x^4\rangle = \langle s_y^4\rangle = \frac{1}{4}\langle(1 - 2s_z^2 + s_z^4)\rangle = \frac{1}{4}\langle(1 - s_z^2)^2\rangle$ and consequently $Z_\perp^{(2)}$ becomes

$$Z_\perp^{(2)} = \tfrac{1}{2}Z_0^{(0)} - Z_\parallel^{(1)} + \tfrac{1}{2}Z_\parallel^{(2)}.$$

Inserting this result back into Eq. (15) and using Eq. (A4), we rewrite the partition function Z in terms of $Z_\parallel^{(0)}$ and its derivatives with respect to σ ($\partial_\sigma^n Z_\parallel^{(0)}$),

$$Z \simeq Z_\parallel^{(0)} + \frac{\sigma\zeta}{2}\left\{(\partial_\sigma Z_\parallel^{(0)}) - \frac{1}{2}\left[Z_\parallel^{(0)} + 3\left(\partial_\sigma^2 Z_\parallel^{(0)}\right)\right]\right\}. \tag{16}$$

This can further be rewritten in terms of Legendre polynomials as follows:

$$Z \simeq Z_\parallel^{(0)}\left\{1 - \sigma\zeta\left[\frac{7}{30} + \frac{2}{21}\mathcal{C}_2 + \frac{6}{35}\mathcal{C}_4\right]\right\} \tag{17}$$

with $\mathcal{C}_2$ and $\mathcal{C}_4$ being given in Eq. (A2).

Now the magnetization can be computed from the partition function using $m^{(0)} = \frac{1}{Z}\partial Z/\partial x$. Unfortunately, this leads to a cumbersome expression that we omit here. Representative magnetization curves for two signs of the cubic anisotropy are shown in Fig. 2. We see that for negative (positive) ζ, the nanoparticle assembly is easier (harder) to magnetize than in the case with only uniaxial anisotropy.

Similarly to what was done in Sec. III for the OSP model, one can establish for the EOSP model analytical asymptotes in various field and anisotropy regimes. In the limit $\sigma \gg 1$,

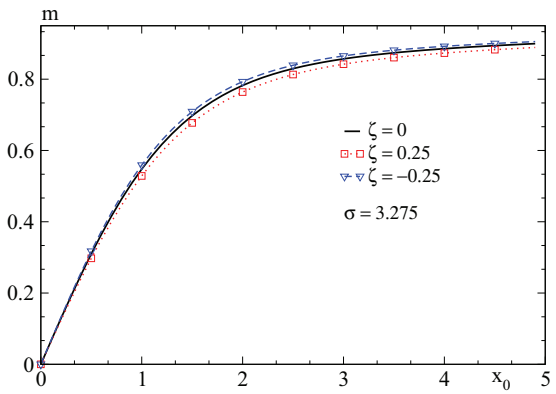

FIG. 2. (Color online) Magnetization as a function of the (dimensionless) field $x_0 = \frac{\mu_B H}{k_B T}$ at temperature $T = 5$ K and various cubic anisotropy values $\zeta = K_4/K_2$.

the partition function $Z_\parallel^{(0)}$ reads [see Eq. (2.74) of Ref. 51 for the case $\zeta = 0$ and arbitrary field]

$$Z_\parallel^{(0)} = \frac{e^\sigma}{\sigma}\cosh x\left\{1 + \frac{1}{2\sigma}(1 - x\tanh x) + \frac{1}{4\sigma^2}[(3 + x^2) - 3x\tanh x]\right\}.$$

Then, substituting the latter in Eq. (16) and performing a double expansion with respect to x for low fields and $1/\sigma$ for high anisotropy leads to the following expression for the magnetization within the EOSP approach:

$$m^{(0)}(x,\sigma,\zeta) \simeq \left(1 - \frac{1}{\sigma}\right)x - \left(1 - \frac{2}{\sigma}\right)\frac{x^3}{3} + \frac{\zeta}{\sigma}\left[-\left(1 - \frac{2}{\sigma}\right)x + \left(2 - \frac{5}{\sigma}\right)\frac{x^3}{3}\right]. \tag{18}$$

This can also be rewritten in the form $m^{(0)} \simeq \chi^{(1)}x + \chi^{(3)}x^3$, where one can easily identify the EOSP corrections to the linear and cubic susceptibilities (in the limit of high-anisotropy barrier) corrected by surface anisotropy,

$$\chi^{(1)} \simeq \left(1 - \frac{1}{\sigma}\right) + \frac{\zeta}{\sigma}\left(-1 + \frac{2}{\sigma}\right), \qquad \chi^{(3)} \simeq \frac{1}{3}\left[\left(-1 + \frac{2}{\sigma}\right) + \frac{\zeta}{\sigma}\left(2 - \frac{5}{\sigma}\right)\right]. \tag{19}$$

The competition between the uniaxial and cubic anisotropy contributions can be understood as follows. As discussed earlier (see also Ref. 35), for $\zeta > 0$ the energy minima of the cubic contribution are along the cube diagonals $[\pm 1, \pm 1, \pm 1]$, while for $\zeta < 0$ they are along the cube edges $[1,0,0]$,$[0,1,0]$,$[0,0,1]$. Hence, the uniaxial anisotropy with an easy axis along the z direction, i.e., $[0,0,1]$, competes with the cubic anisotropy when $\zeta > 0$, whereas the two anisotropies have a concomitant effect when $\zeta < 0$. In the former case, the particle's magnetic moment at equilibrium takes an intermediate direction between the z axis and the cube diagonal. Hence, as ζ increases, the magnetic moment gradually rotates away from the z axis and thereby its statistical average, or the magnetization, decreases. In the case of

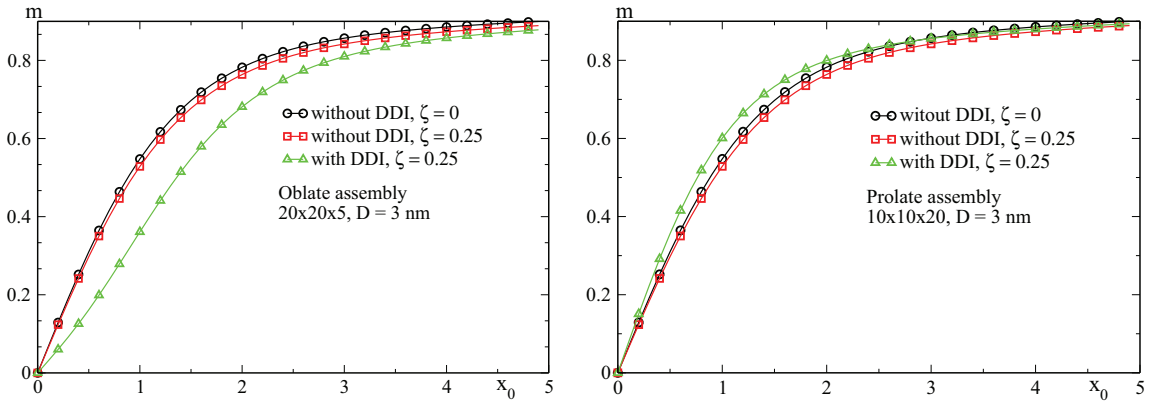

FIG. 3. (Color online) Left: magnetization as a function of the (dimensionless) field $x_0 = \frac{\mu_B H}{k_B T}$ for an oblate sample ($20 \times 20 \times 5$). Right: the same for a prolate sample ($10 \times 10 \times 20$). Here, for both panels $\sigma = 3.275$ and when the dipolar interaction is switched on $\xi \simeq 0.18$ corresponding to a volume concentration $C_v = 0.24\%$.

negative ζ, the two anisotropies cooperate to quickly drive the magnetization toward saturation.

B. Surface effects in the presence of DDIs

Finally, we derive the asymptotic expressions for the magnetization, taking into account both surface anisotropy and DDIs, in addition of course to the contributions from the uniaxial anisotropy and magnetic field. Accordingly, using the asymptotic expression (19) in Eq. (10) leads to

$$m(x,\sigma,\zeta,\tilde{\xi}) \simeq \tilde{\chi}^{(1)} x + \tilde{\chi}^{(3)} x^3, \tag{20}$$

where

$$\begin{aligned} \tilde{\chi}^{(1)} &\simeq \chi^{(1)} + \tilde{\xi}\left[1 - \frac{2}{\sigma} - 2\left(1 - \frac{3}{\sigma}\right)\frac{\zeta}{\sigma}\right], \\ \tilde{\chi}^{(3)} &\simeq \chi^{(3)} - \frac{4}{3}\tilde{\xi}\left[\left(1 - \frac{3}{\sigma}\right) - \frac{3\zeta}{\sigma}\right] \end{aligned} \tag{21}$$

are the linear and cubic susceptibilities of Eq. (19) corrected by DDIs.

This is an important result of this work that is directly related to its title. Indeed, this asymptotic expression allows us to figure out how surface anisotropy competes with DDIs. More precisely, the sign of the surface contribution with intensity ζ plays an important role in the magnetization curve. Yet, as it couples to the DDI $\tilde{\xi}$ parameter, which contains information on the sample's shape, it is the overall sign of $\tilde{\xi}\zeta$ that determines whether there is a competition between surface and DDI effects or whether the changes in magnetization induced by the intrinsic and collective contributions have the same tendency. The answer is given in the following discussion.

Plots of the magnetization, which take into account both surface effects and DDIs, are shown in Fig. 3 as a function of the (dimensionless) field x for an oblate sample with $N_x \times N_y \times N_z = 20 \times 20 \times 5$ and a prolate sample with $10 \times 10 \times 20$, with the corresponding values of $\mathcal{C}^{(0,0)} \simeq -4.0856$ and 1.7293, respectively. For larger systems, with the same aspect ratios, one obtains, according to Ref. 52, $\mathcal{C}^{(0,0)} \simeq -3.9868$ and 1.69662. For a given sign of ζ, the figure shows the role of the sample's geometry: while the intrinsic surface effects are always demagnetizing in the present case with $\zeta > 0$, the DDIs can either contribute positively (prolate sample) or negatively (oblate sample) to the magnetization.

For maghemite nanoparticles, it was observed that for dilute assemblies of very small particles (of 3 nm in diameter) the magnetization curves $m(H)$ at different temperatures showed a kind of a "fanning out" as the temperature dropped below some value (approximately 100 K); see Fig. 3 of Ref. 8. The magnetization enhancement at low temperature strongly depends on the particles size and was thus attributed to surface effects on account of various experiments and numerical simulations.[54] However, as the concentration increases, this fanning vanishes thus recovering the usual magnetization curves $m(H)$ with regular spacing at different temperatures; see Fig. 5 of Ref. 8. This means that DDIs, which become stronger in more concentrated assemblies, seem to "screen out" surface effects and thus to compensate for them (see the discussion in Ref. 10). In fact, this compensation is only partial because the magnetization still does not saturate at the highest field available, as can be seen in Fig. 5 of Ref. 8. In light of the present calculations, the results of Ref. 8 (see also Ref. 24) seem to imply that DDIs have an opposite effect to that of surface anisotropy, represented here by the contribution in ζ. More precisely, according to Eqs. (20) and (21), this implies that the product $\tilde{\xi}\zeta$ is negative, and considering the fact that $\tilde{\xi} < 0$ for oblate samples, the results in Ref. 8 would imply that $\zeta > 0$. Note, however, that the comparison of the present calculations and the experimental results[8] is done with a little daring because the measurements of Ref. 8 were done on thin disk-shaped (hence oblate) samples with the magnetic field applied along the sample plane. In addition, the particles' effective anisotropy easy axes are randomly distributed.

As discussed in the Introduction, this result may help in optimizing the physical parameters (size, shape, concentration, etc.) in view of further fundamental investigations, e.g., of the dynamical properties and the effect of surface anisotropy.

V. DISCUSSION

Now we present and discuss plots of the magnetization for assemblies with varying parameters. First, we discuss the effect of DDIs alone, without surface effects ($\xi \neq 0$, $\zeta = 0$). Next, we comment on the plots of the EOSP calculations of

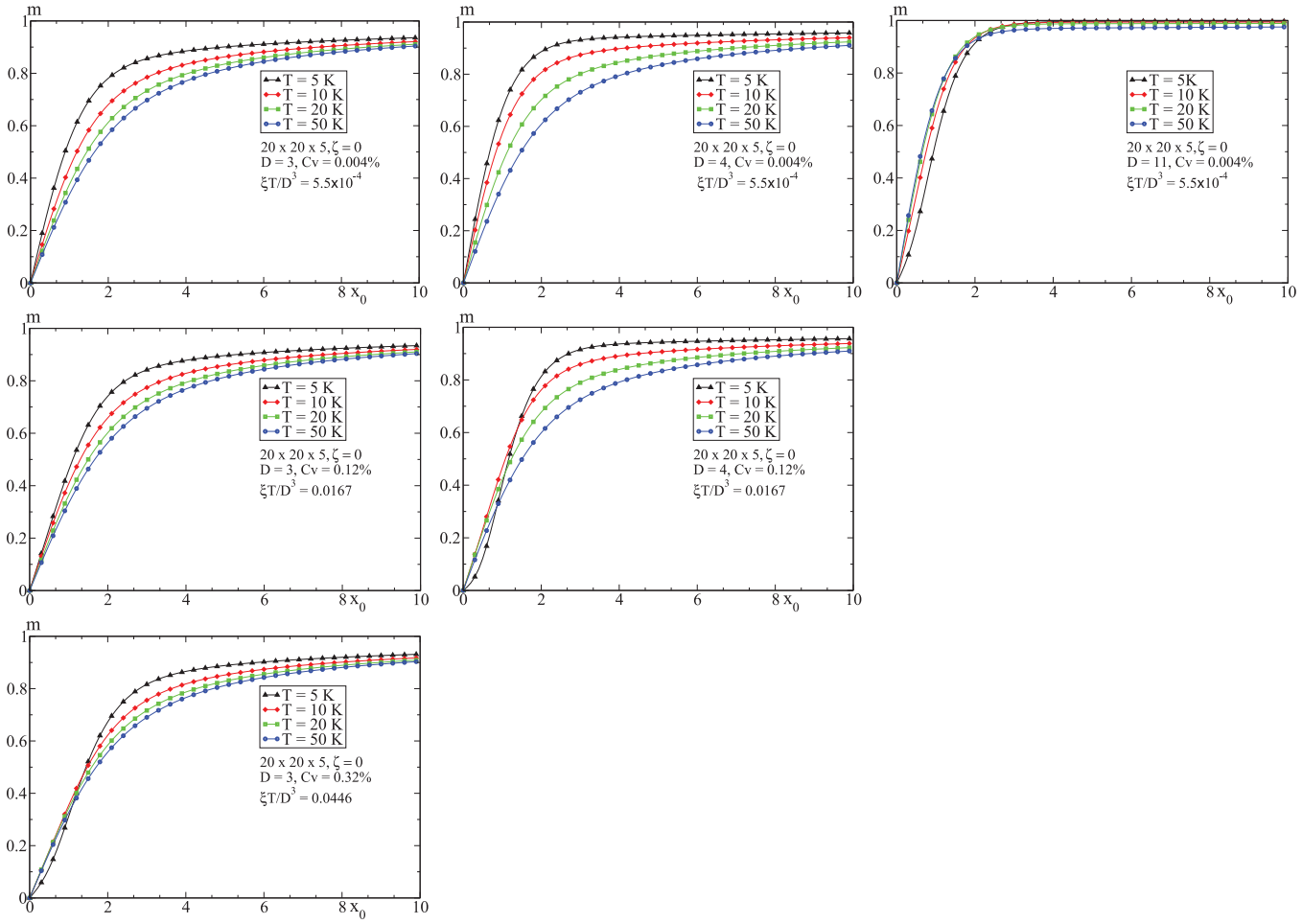

FIG. 4. (Color online) Magnetization curves of an oblate sample ($20 \times 20 \times 5$) as a function of the (dimensionless) field $x_0 = \frac{\mu_B H}{k_B T}$, for different temperatures T, different particle diameters D (in nm), and different volume concentrations C_v, without surface effects ($\zeta = 0$ and $\xi \neq 0$). Since the reduced (uniaxial) anisotropy σ depends on both the temperature and the particle diameter, the calculations presented in these panels are done for a constant value of $\frac{\sigma T}{D^3} \simeq 0.6066$ K nm^{-3}. Similarly, for each line the dipolar parameter $\frac{\xi T}{D^3}$ is expressed in the same units. The upper panel with a very low concentration ($C_v = 0.004\%$) corresponds to an interparticle distance of $a \simeq 15.3D$, while the highest concentration in the lower panel ($C_v = 0.32\%$) leads to $a \simeq 3.5D$.

Sec. IV showing the combined effects of DDIs and surface anisotropy ($\xi \neq 0, \zeta \neq 0$).

A. Effect of dipolar interactions on the magnetization ($\zeta = 0$ and $\xi \neq 0$)

Here we restrict ourselves to the study of the DDI effect ($\xi \neq 0$) on the magnetization of an assembly of monodisperse magnetic nanoparticles, ignoring for the time being the effect of surface anisotropy ($\zeta = 0$). The results of magnetization curves at different temperatures for assemblies with different concentrations (increasing downward) and particle diameters (increasing from left to right) are shown in Fig. 4.

The upper right panel displays the magnetization curves of an assembly with a volume concentration $C_v = 0.004\%$ and a particle diameter $D = 11$ nm. In this case, we see that the saturation is obviously easier at lower temperatures. For a given concentration, upon increasing the diameter of the particles (thus moving to the right within the same row), we see that the magnetization curves saturate more quickly (in lower fields) since for larger particles, the Zeeman energy ($\mathcal{E}_{\text{Zeeman}} \propto \mathbf{m} \cdot \mathbf{H}$ with $m \propto n_i$) is larger and thence the magnetizing effect of the external field is bigger. On the other hand, for a given particle diameter, an increase of the particle concentration C_v (going downward within the same column) reduces the interparticle distance a and thus increases the DDI parameter $\tilde{\xi}$. For the oblate sample considered here, the DDIs tend to maintain the magnetic moments in the xy plane and thus oppose the effect of the external magnetic field. This competition is reflected in the magnetization curves by the appearance of an inflection point which is marked by the black curves in Fig. 4, i.e., for $T = 5$ K. This feature becomes obvious by looking at the susceptibility, namely dm/dx_0, as displayed in Fig. 5.

The results are in agreement with the low-field expansion (20), which reads (for $\zeta = 0$)

$$m \simeq \left(1 - \frac{1}{\sigma}\right) x - \left(1 - \frac{2}{\sigma}\right) \frac{x^3}{3} + \tilde{\xi} \left[\left(1 - \frac{2}{\sigma}\right) x - 4 \left(1 - \frac{3}{\sigma}\right) \frac{x^3}{3} \right].$$

Indeed, at low fields the first line (corresponding to free particles) in this expression goes above the one between the square brackets when both are plotted against the field. As such, as the concentration increases, $\tilde{\xi}$ increases and the effect of DDIs tends to depress the magnetization. We may use different terms to interpret the appearance of the inflection point for constant volume concentration C_v when D is increased, as is the case when comparing the $T = 5$ K curves of the upper panels in Fig. 4. Going to larger particles increases $\tilde{\xi}$, which leads to a sign change of the second derivative of m with respect to the field as it can be inferred from the expression above. This well-marked feature in the magnetization curve can be viewed as a signature of the dipolar interaction in textured oblate assemblies. In the case of a prolate sample, the DDIs induce an anisotropy that adds up to the magnetocrystalline anisotropy that is intrinsic to the particles. Consequently, there is no competition between DDIs and the latter.

B. Effective model EOSP ($\zeta \neq 0$ and $\xi \neq 0$)

To take into account surface effects, we include the effective anisotropy contribution ($\zeta \neq 0$) according to the EOSP model. We will show here that depending on the sign of ζ, we can have concomitant or competing effects between surface and dipolar contributions.

We have assumed DDIs to be relatively weak so that we can use perturbation theory to derive an analytical expression for the magnetization. As such, we have to content ourselves with a small effect of DDIs. To understand their interplay with surface effects, we have studied the behavior of a physical quantity for which their effect is more explicit. As mentioned earlier, it happens that the magnetization curves present an inflection point that can be more clearly appreciated by examining the derivative of these curves. This derivative turns out to exhibit a maximum at some reduced field x_{inf}. We show an example of this in Fig. 5, where the inflection point appears at $x_{\text{inf}} \approx 0.8$ for the given parameters.

We then extract x_{inf} (or H_{inf}) and plot it as a function of the concentration, or equivalently the DDI coefficient $\tilde{\xi}$. This is shown in Fig. 6, which applies to a monodisperse assembly of nanoparticles with diameter $D = 3$ nm at $T = 5$ K, for a sample of size ($20 \times 20 \times 5$). There are three curves: one for

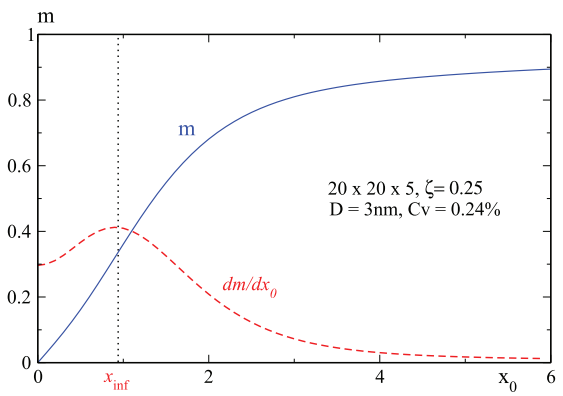

FIG. 5. (Color online) Magnetization and its derivative as functions of the (dimensionless) field $x_0 = \frac{\mu_B H}{k_B T}$ and its derivative for an oblate assembly at $T = 5$ K.

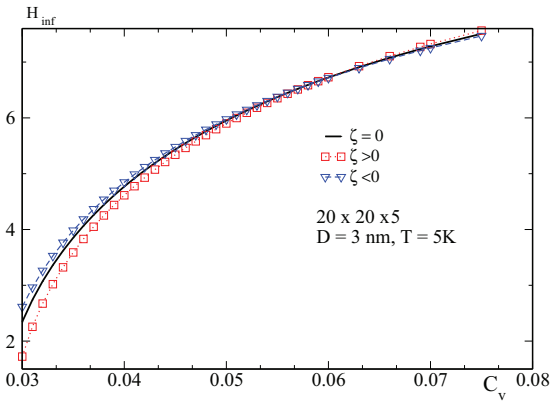

FIG. 6. (Color online) Field H_{inf} as a function of C_v for a monodisperse oblate ($20 \times 20 \times 5$) assembly with $D = 3$ nm and $T = 5$ K.

$\zeta = 0$, for which surface effects are dropped, one for $\zeta < 0$, and the other for $\zeta > 0$, for which surface effects play opposite roles. The change of sign of ζ can be achieved experimentally due to the fact that, depending on the material chosen for the particles and their size and shape, the effective anisotropy can change sign.

In Fig. 6, we first see that H_{inf} increases with C_v as expected for all cases since then the DDIs become stronger and the competition with the external magnetic field becomes more pronounced. Let us compare the curve $\zeta < 0$ to that with $\zeta = 0$, keeping in mind our discussion of the effects of cubic anisotropy. The various contributions to the energy are (i) the uniaxial anisotropy with an easy axis along the z axis, (ii) the cubic anisotropy for which the easy axes are along x, y, and z for $\zeta < 0$, (iii) the external magnetic field along z, and (iv) DDIs, which tend to place the magnetic moments in the xy plane for an oblate sample ($\zeta < 0$).

For low concentrations, the uniaxial and cubic anisotropies are the most dominant contributions to the energy. The three directions x,y, and z are degenerate with respect to the cubic anisotropy, but since the z axis is favored by the uniaxial anisotropy, this direction is selected. For this reason, the field H_{inf} is larger if $\zeta < 0$. On the contrary, for high concentrations the DDI contribution is predominant and its effect is concomitant with that of the cubic anisotropy. Again, the directions x, y, and z are degenerate with respect to the cubic anisotropy, but this time the xy plan is favored by DDIs. It is therefore more difficult to drive the magnetization out of the xy plane, and this explains why H_{inf} becomes lower than for the $\zeta = 0$ case above some value of C_v.

For a more systematic study, we compared an oblate ($20 \times 20 \times 5$) with a prolate ($10 \times 10 \times 20$) sample. The results are shown in Fig. 7, where the magnetization is plotted as a function of the field x. We consider different concentrations C_v and different situations with respect to surface effects by choosing either $\zeta > 0$ or $\zeta < 0$. As a reference, we also plot the curve corresponding to free particles ($C_v \sim 0$) with and without surface effects ($\zeta = 0$).

For the oblate sample ($20 \times 20 \times 5$), the easy plane for DDIs is the xy plane. The upper left graph of Fig. 7 corresponds to $\zeta > 0$, for which the cubic anisotropy easy axes are along the main diagonals of the cube. DDIs and surface effects cooperate

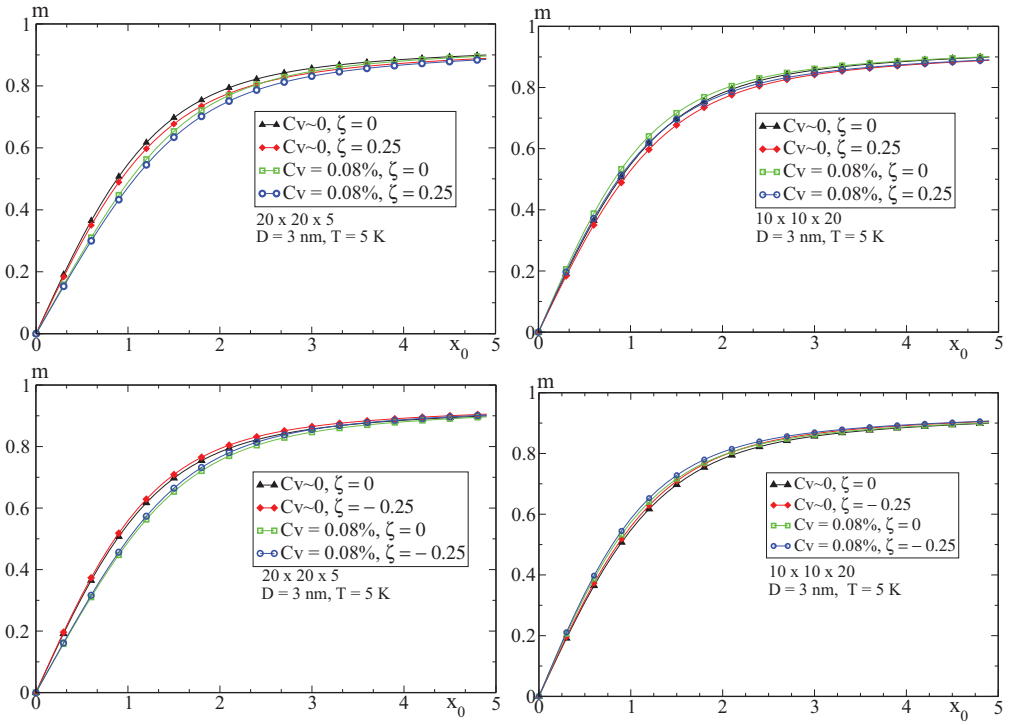

FIG. 7. (Color online) Magnetization as a function of the (dimensionless) field x_0 for assemblies of monodisperse particles of diameter $D = 3$ nm at (constant) temperature $T = 5$ K. Left column: oblate ($20 \times 20 \times 5$) sample. Right column: prolate ($10 \times 10 \times 20$) sample.

to suppress the magnetization leading to a magnetization curve that remains below the reference curve. The graph at the bottom left of Fig. 7 represents the case with $\zeta < 0$. We observe in this case a competition between DDIs and surface effects.

For the prolate sample ($10 \times 10 \times 20$), the opposite effect is observed. Indeed, this time the z axis is favored by DDIs. If $\zeta < 0$, as shown in the bottom right of Fig. 7, the z axis is selected by both DDIs and surface anisotropy. Hence, the magnetization curves fall above the reference curve and thus the magnetization of the assembly is enhanced.

VI. CONCLUSION AND OUTLOOK

In this work, we have examined in detail the competition between intrinsic effects and collective behavior in an assembly of (weakly) interacting nanoparticles. To account for surface effects, we have adopted the effective one-spin problem that represents a nanoparticle as a macroscopic magnetic moment evolving in an effective energy potential which is a polynomial in the components of the particle's net magnetic moment. The coefficients of this potential change in sign and magnitude with the underlying lattice, the size, and the shape of the particles.

This, in conjunction with the use of perturbation theory, has allowed us to derive sensible analytical expressions for the magnetization of a nanoparticle within the assembly that include the applied magnetic field, the core and surface anisotropy, and the dipole-dipole interactions.

Given the fact that (i) the DDI contribution changes sign according to the shape of the assembly and (ii) the surface-anisotropy contribution also changes sign and magnitude upon changing the underlying lattice, the size, and the shape of the particles, it is possible to design samples for which various situations can be encountered with either competing or concomitant effects. In Ref. 53 it was shown that as the surface anisotropy increases, the magnetization relaxation rate evolves through a bell-shaped curve, which means that there is a range of physical parameters (lattice, size, shape, surface morphology) for which the relaxation rate is maximal or the relaxation time is the shortest. This implies that for such parameters, the particle magnetization is least stable against thermal fluctuations. Now, nanoparticles with physical parameters outside this range may be organized or assembled in such a way that the dipole-dipole interactions acquire a concomitant effect that eventually leads to an assembly with higher and more stable magnetization. This is one of the main features sought for future applications, e.g., in the area of magnetic recording.

From the standpoint of fundamental research, we hope that this work sheds light on the behavior of such a complex system as an interacting assembly of nanoparticles whose intrinsic features are accounted for to some extent. Indeed, the analytical expressions for the magnetization, established in various typical realistic regimes, are a handy tool for further investigations of the effects of the various physical parameters involved. Likewise, they will be quite useful in accompanying the near future numerical simulations using the Monte Carlo technique that we have planned and in which we intend to test this competition between surface anisotropy and dipolar interactions. More precisely, we consider an assembly of a small number of nanoclusters modeled as many-spin systems. The idea behind this work is, in addition to a comparison with the analytical work developed here, to explore the regime of stronger dipolar interactions and to assess the limit of validity of the results presented here.

The effects of surface anisotropy on the dynamics of a nanoparticle assembly are one of the still appealing topics, with a plethora of physical phenomena awaiting more thorough investigation. Accordingly, we are planning equilibrium and dynamical measurements on chains of iron nanoparticles with controlled size and separation.[55,56] One of the issues we would like to investigate is related to the effect of particle separation on the low- and high-frequency dynamics of the nanoparticles. The results of the present work will be extremely helpful in this endeavor.

ACKNOWLEDGMENTS

We would like to thank Denis Ledue for fruitful discussions of dipolar interaction in assemblies of magnetic nanoparticles. O.I. acknowledges funding by the Spanish MINECO (MAT2009-0667 and MAT2012-33037), Catalan DURSI (2009SGR856), and European Union FEDER funds (Una manera de hacer Europa). He also acknowledges CESCA and CEPBA under coordination of C4 for supercomputer facilities.

APPENDIX: MAGNETIZATION AND HIGH-ORDER CORRELATIONS

We give here some details of the calculation of the equilibrium magnetization for the EOSP model without DDIs. Using the Legendre polynomials, $p_n(z)$ [$p_1(z) = z$, $p_2(z) = \frac{1}{2}(3z^2 - 1)$, $p_4(z) = \frac{1}{8}(35x^4 - 30x^2 + 3), \dots$] we define the anisotropy-weighted averages

$$\mathcal{C}_n(\sigma,x) = \langle p_n(z)\rangle_0 = \int_{-1}^{1} dz\, \mathcal{P}_0(z)\; p_n(z)\,. \tag{A1}$$

Let us also define the equivalent averages at zero field, i.e., $S_n(\sigma) \equiv \mathcal{C}_n(\sigma,0)$. One finds

$$\langle s_z\rangle_0 = \mathcal{C}_1, \quad \langle s_z^2\rangle_0 = \tfrac{1}{3}(1 + 2\mathcal{C}_2)\,,$$
$$\langle s_{x,y}\rangle_0 = 0, \quad \langle s_{x,y}^2\rangle_0 = \tfrac{1}{3}(1 - \mathcal{C}_2)$$

with

$$\begin{aligned}
\mathcal{C}_1 &= \frac{e^\sigma}{\sigma Z_\parallel^{(0)}}\sinh x - h = m^{(0)},\\
\mathcal{C}_2 &= \frac{3}{2}\left[\frac{e^\sigma}{\sigma Z_\parallel^{(0)}}(\cosh x - h\sinh x) + h^2 - \frac{1}{2\sigma}\right] - \frac{1}{2},\\
\mathcal{C}_4 &= \frac{3}{2}\frac{1}{Z_\parallel^{(0)}\sigma}\left[\left(2\exp\sigma - \mathcal{C}_2 - \frac{1}{\sigma}\right)\cosh x\right]\\
&\quad + \frac{3}{4}\frac{x\sinh x}{Z_\parallel^{(0)}\sigma}\left[\mathcal{C}_2 + \frac{1}{\sigma}\right] + \frac{3}{2}\left[\frac{x^2}{3\sigma^3} + \frac{1}{2\sigma^2}\right].
\end{aligned} \tag{A2}$$

Then the (reduced) equilibrium susceptibility tensor is defined as

$$\chi_{\alpha\beta} = \langle s_\alpha s_\beta\rangle_0 - \langle s_\alpha\rangle_0\langle s_\beta\rangle_0,$$
$$\chi_\parallel = \chi_{zz}, \quad \chi_\perp = \chi_{xx} = \chi_{yy}.$$

Using the definitions given above, the (reduced) static susceptibility components read

$$\chi_\parallel = \frac{1 + 2S_2}{3} - S_1^2, \qquad \chi_\perp = \frac{1 - S_2}{3}. \tag{A3}$$

We then define

$$Z_\parallel^{(n)} \equiv \int s_z^{2n} d\omega^{(0)} = \frac{\partial^n Z_\parallel^{(0)}}{\partial\sigma^n} \tag{A4}$$

and write the first two derivatives of $Z_\parallel^{(0)}$ with respect to σ, i.e., $Z_\parallel^{(1)}, Z_\parallel^{(2)}$, in terms of the averages of Legendre polynomials as follows:

$$\begin{aligned}
Z_\parallel^{(1)} &= \int s_z^2 d\omega^{(0)} = \frac{Z_\parallel^{(0)}}{3}(2\mathcal{C}_2 + 1)\,,\\
Z_\parallel^{(2)} &= \int s_z^4 d\omega^{(0)} = \frac{Z_\parallel^{(0)}}{35}[8\mathcal{C}_4 + 20\mathcal{C}_2 + 7]\,.
\end{aligned} \tag{A5}$$

$\partial^2 Z_0^{(0)}/\partial\sigma^2$ is simply the derivative of $\chi_\parallel$ above with respect to σ. In the absence of the field, the averages $\mathcal{C}_2$ and $\mathcal{C}_4$ become the "anisotropy functions" S_2 and S_4 which have the asymptotes[51]

$$S_l(\sigma) \simeq \begin{cases} \frac{2^{l/2}(l-1)!!}{(2l+1)!!}\sigma^{l/2} + \cdots, & \sigma \ll 1,\\ 1 - \frac{l(l+1)}{4\sigma} + \cdots, & \sigma \gg 1. \end{cases} \tag{A6}$$

For the calculation of the field and anisotropy asymptotes, we seek an expansion of the magnetization in the low-field regime as

$$m \simeq \chi^{(1)}x + \chi^{(3)}x^3, \tag{A7}$$

where[31] the coefficient of the linear contribution reads

$$\chi^{(1)} = a_0^{(1)} + a_1^{(1)}\xi + a_2^{(1)}\xi^2 \tag{A8}$$

with

$$\begin{aligned}
a_0^{(1)} &= \frac{1 + 2S_2}{3}, \quad a_1^{(1)} = a_0^2\mathcal{C}^{(0,0)},\\
a_2^{(1)} &= -\frac{2a_0^2}{3}[(1 - S_2)(\bar{\mathcal{R}} - \mathcal{S}) + 3S_2(\mathcal{T} - \mathcal{U})]\\
&\quad + \frac{b_0}{2}\left[(1 - S_2)\mathcal{V} + 3S_2\left(\mathcal{T} - \frac{1}{3}\bar{\mathcal{R}}\right)\right],\\
b_0 &= \frac{4}{315}\left(7 + 10S_2 - 35S_2^2 + 18S_4\right).
\end{aligned} \tag{A9}$$

Here, $\mathcal{C}^{(0,0)}, \bar{\mathcal{R}}, \mathcal{S}, \mathcal{T}, \mathcal{U}, \mathcal{V}$ are certain lattice sums discussed in Ref. 31.

The coefficient of the cubic contribution is given here only up to first order in ξ,

$$\chi^{(3)} = a_0^{(3)}\left[1 + \xi 4\mathcal{C}^{(0,0)}a_0^{(1)}\right], \tag{A10}$$

where

$$a_0^{(3)} = -\frac{1}{315}\left(7 + 40S_2 + 70S_2^2 - 12S_4\right).$$

Inserting the low- and high-field anisotropy expressions for $S_l(\sigma)$ into the coefficients of Eq. (A9) and then substituting the corresponding low- and high-field expansions of the Langevin function leads to the asymptotic equations of the main text.

*francois.vernay@univ-perp.fr
†oscariglesias@ub.edu

[1]M. P. Sharrock, IEEE Trans. Magn. **26**, 193 (1990).
[2]K. E. Johnson, J. Appl. Phys. **69**, 4932 (1991).
[3]J.-L. Dormann, D. Fiorani, and E. Tronc, Adv. Chem. Phys. **98**, 283 (1997).
[4]X. Batlle and A. Labarta, J. Phys. D **35**, R15 (2002).
[5]P. Tartaj, M. del Puerto Morales, S. Veintemillas-Verdaguer, T. González-Carreño, and C. J. Serna, J. Phys. D **36**, R182 (2003).
[6]J. P. Chen, C. M. Sorensen, K. J. Klabunde, and G. C. Hadjipanayis, Phys. Rev. B **51**, 11527 (1995).
[7]M. Respaud, J. M. Broto, H. Rakoto, A. R. Fert, L. Thomas, B. Barbara, M. Verelst, E. Snoeck. P. Lecante, A. Mosset, J. Osuna, T. O. Ely, C. Amiens, and B. Chaudret, Phys. Rev. B **57**, 2925 (1998).
[8]E. Tronc, A. Ezzir, R. Cherkaoui, C. Chanéac, M. Noguès, H. Kachkachi, D. Fiorani, A. M. Testa, J. M. Grenèche, and J. P. Jolivet, J. Magn. Magn. Mater. **221**, 63 (2000).
[9]H. Kachkachi and D. A. Garanin, in *Surface Effects in Magnetic Nanoparticles*, edited by D. Fiorani (Springer, Berlin, 2005), p. 75.
[10]H. Kachkachi, in *Nanomagnet Embedded in Matrix (NEIM)*, edited by V. Dupuis (Transworld Research Network, Kerala, 2005), p. 1.
[11]R. H. Kodama, A. E. Berkowitz, E. J. McNiff, and S. Foner, Phys. Rev. Lett. **77**, 394 (1996).
[12]F. Gazeau, E. Dubois, M. Hennion, R. Perzynski, and Yu. Raikher, Europhys. Lett. **40**, 575 (1997).
[13]R. H. Kodama, S. A. Makhlouf, and A. E. Berkowitz, Phys. Rev. Lett. **79**, 1393 (1997).
[14]S. Morup and E. Tronc, Phys. Rev. Lett. **72**, 3278 (1994).
[15]C. Petit, A. Taleb, and M.-P. Pileni, Adv. Mater. **10**, 259 (1998).
[16]V. P. Shilov, Y. L. Raikher, J.-C. Bacri, F. Gazeau, and R. Perzynski, Phys. Rev. B **60**, 11902 (1999).
[17]M. Respaud, M. Goiron, J. M. Broto, F. H. Yang, T. O. Ely, C. Amiens, and B. Chaudret, Phys. Rev. B **59**, R3934 (1999).
[18]S. Sun and C. B. Murray, J. Appl. Phys **85**, 4325 (1999).
[19]F. Luis, F. Petroff, and J. Bartolomé, J. Phys.: Condens. Matter **16**, 5109 (2004).
[20]E. De Biasi, R. D. Zysler, C. A. Ramos, H. Romero, and D. Fiorani, Eur. Phys. J. B **51**, 65 (2006).
[21]J. S. Lee, R. P. Tan, J. H. Wu, and Y. K. Kim, Appl. Phys. Lett. **99**, 062506 (2011).
[22]V. Russier, C. de Montferrand, Y. Lalatonne, and L. Motte, J. Appl. Phys. **112**, 073926 (2012).
[23]A. Ezzir, Ph.D. thesis, Université Paris–Sud, Orsay, 1998.
[24]H. Kachkachi, A. Ezzir, M. Noguès, and E. Tronc, Eur. Phys. J. B **14**, 681 (2000).
[25]H. Kachkachi, W. T. Coffey, D. S. F. Crothers, A. Ezzir, E. C. Kennedy, M. Noguès, and E. Tronc, J. Phys.: Condens. Matter **12**, 3077 (2000).
[26]D. Kechrakos and K. N. Trohidou, Phys. Rev. B **58**, 12169 (1998).
[27]V. Russier, C. Petit, J. Legrand, and M.-P. Pileni, Appl. Surf. Sci. **164**, 193 (2000).
[28]J. Garcia-Otero, M. Porto, J. Rivas, and A. Bunde, Phys. Rev. Lett. **84**, 167 (2000).
[29]P. E. Jonsson and J. L. Garcia-Palacios, Europhys. Lett. **55**, 418 (2001).
[30]D. V. Berkov and N. L. Gorn, J. Phys.: Condens. Matter **13**, 9369 (2001).
[31]P. E. Jonsson and J. L. Garcia-Palacios, Phys. Rev. B **64**, 174416 (2001).
[32]H. Kachkachi and M. Azeggagh, Eur. Phys. J. B **44**, 299 (2005).
[33]M. Azeggagh and H. Kachkachi, Phys. Rev. B **75**, 174410 (2007).
[34]H. Kesserwan, G. Manfredi, J. Y. Bigot, and P.-A. Hervieux, Phys. Rev. B **84**, 172407 (2011).
[35]G. Margaris, K. N. Trohidou, and H. Kachkachi, Phys. Rev. B **85**, 024419 (2012).
[36]D. Ledue, R. Patte, and H. Kachkachi, J. Nanosci. Nanotechnol. **12**, 4953 (2012).
[37]G. Landi, J. Appl. Phys. **113**, 163908 (2013).
[38]J. L. Dormann, L. Bessais, and D. Fiorani, J. Phys. C **21**, 2015 (1988).
[39]H. Mamiya and I. Nakatani, J. Magn. Magn. Mater. **177**, 966 (1998).
[40]J.-L. Dormann and D. Fiorani, J. Magn. Magn. Mater. **202**, 251 (1999).
[41]P. Allia, M. Coisson, P. Tiberto, F. Vinai, M. Knobel, M. A. Novak, and W. C. Nunes, Phys. Rev. B **64**, 144420 (2001).
[42]H. Mamiya, I. Nakatani, and T. Furubayashi, Phys. Rev. Lett. **88**, 067202 (2002).
[43]Ò. Iglesias and A. Labarta, Phys. Rev. B **70**, 144401 (2004).
[44]O. Chubykalo-Fesenko and R. W. Chantrell, J. Appl. Phys. **97**, 10J315 (2005).
[45]S. H. Masunaga, R. F. Jardim, P. F. P. Fichtner, and J. Rivas, Phys. Rev. B **80**, 184428 (2009).
[46]A. F. Franco, J. M. Martinez, J. L. Déjardin, and H. Kachkachi, Phys. Rev. B **84**, 134423 (2011).
[47]D. A. Garanin and H. Kachkachi, Phys. Rev. Lett. **90**, 065504 (2003).
[48]H. Kachkachi and E. Bonet, Phys. Rev. B **73**, 224402 (2006).
[49]R. Yanes, O. Chubykalo-Fesenko, H. Kachkachi, D. A. Garanin, R. Evans, and R. W. Chantrell, Phys. Rev. B **76**, 064416 (2007).
[50]H. Kachkachi, J. Magn. Magn. Mater. **316**, 248 (2007).
[51]J. L. Garcia-Palacios, Adv. Chem. Phys. **112**, 1 (2000).
[52]A. Aharoni, J. Appl. Phys. **83**, 3432 (1998).
[53]P.-M. Déjardin, H. Kachkachi, and Yu. Kalmykov, J. Phys. D **41**, 134004 (2008).
[54]H. Kachkachi, M. Noguès, E. Tronc, and D. A. Garanin, J. Magn. Magn. Mater. **221**, 158 (2000).
[55]D. Toulemon, B. Pichon, X. Cattoen, M. W. C. Man, and S. Begin-Colin, Chem. Commun. **47**, 11954 (2011).
[56]M. Pauly, B. P. Pichon, P. Panissod, S. Fleutot, P. Rodriguez, M. Drillon, and S. Begin-Colin, J. Mater. Chem. **22**, 6343 (2012).